appendix

A

Bragg's Diffraction Law and X-ray Diffraction

Bragg's Diffraction Condition

X-rays are electromagnetic (EM) waves with wavelengths typically in the range from 0.01 nm to a few nanometers. This wavelength region is comparable with typical interplanar spacings in crystals. When an X-ray beam impinges on a crystal, the waves in the beam interact with the planes of atoms in the crystal and, as a result, the waves become scattered and the X-ray beam becomes diffracted. An analogy with radio waves may help. Radio waves with wavelengths in the range 1–10 m (short waves and VHF waves) easily interact with objects of comparable size. It is well known that these radio waves become scattered by objects of comparable size such as trees, houses, and buildings. However, long-wave radio waves with wavelengths in kilometers do not become scattered by these objects because the object sizes now are much smaller than the wavelength.

When X-rays strike a crystal, the EM waves penetrate the crystal structure. Each plane of atoms in the crystal reflects a portion of the waves. The reflected waves from different planes then interfere with each other and give rise to a **diffracted beam** which is at a well-defined angle 2θ to the incident beam as depicted in Figure A.1. Some of the incident beam goes through the crystal undiffracted and some of the beam becomes diffracted. Further, the diffracted rays exist only in certain directions. These diffraction directions correspond to well-defined diffraction angles 2θ, as defined in Figure A.1. The diffraction angle 2θ, the wavelength of the X-rays λ, and the interplanar separation d of the diffraction planes within the crystal are related through the **Bragg diffraction condition,** that is,

Bragg's law

$$2d\sin\theta = n\lambda \qquad n = 1, 2, 3, \ldots \tag{A.1}$$

Figure A.1 A schematic illustration of X-ray diffraction by a crystal.
X-rays penetrate the crystal and then become diffracted by a series of atomic planes.

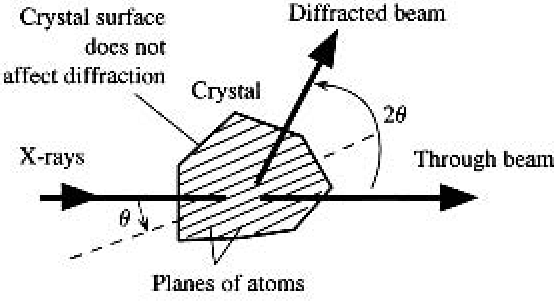

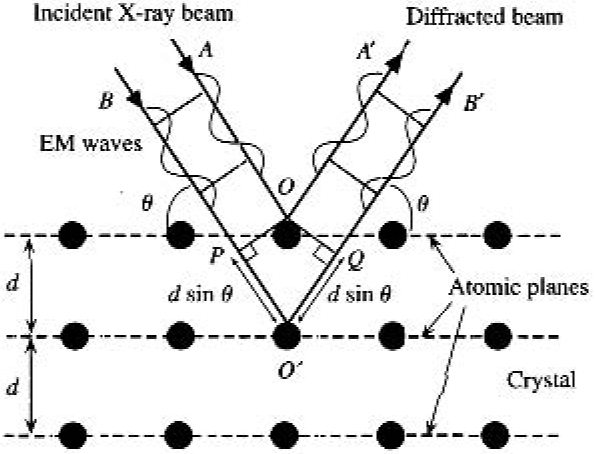

Figure A.2 Diffraction involves X-ray waves being reflected by various atomic planes in the crystal. These waves interfere constructively to form a diffracted beam only for certain diffraction angles that satisfy the Bragg condition.

Consider X-rays penetrating a crystal structure and becoming reflected by a given set of atomic planes as shown in Figure A.2. We can consider an X-ray beam to be many parallel waves that are in phase. These waves penetrate the crystal structure and become reflected at successive atomic planes. The interplanar separation of these planes is d. Waves reflected from adjacent atomic planes interfere constructively to constitute a diffracted beam only when the path difference between the rays is an integer multiple of the wavelength—a requirement of *constructive interference*. This will only be the case for certain directions of reflection. For simplicity, we will consider two waves A and B in an X-ray beam being reflected from two consecutive atomic planes in the crystal. The angle between the X-rays and the atomic planes is θ as defined in Figure A.2. Initially the waves A and B are in phase. Wave A is reflected from the first plane, whereas wave B is reflected from the second plane. When wave A is reflected at O, wave B is at P. Wave B becomes reflected from O' on the second plane and then moves along reflected B'. Wave B has to travel a further distance, $PO'Q$, equivalent to $2d \sin \theta$ before reaching wave A. The path difference between the two reflected waves A' and B' is $PO'Q$ or $2d \sin \theta$. For constructive interference this must be $n\lambda$ where n is an integer. Otherwise the reflected waves will interfere destructively and cancel each other out. Thus the condition for the existence of a diffracted beam is that the path difference between A' and B' should be a multiple of the wavelength λ; which is Equation A.1. The diffraction condition in Equation A.1 is referred to as **Bragg's law.** The angle θ is called the **Bragg angle,** whereas 2θ is called the **diffraction angle.** The index n is called the order of diffraction. The incidence angle θ is the angle between the incident X-ray and the atomic planes within the crystal and not the angle at the actual crystal surface. The crystal surface, whatever shape, does not affect the diffraction process because X-rays penetrate the crystal and then become diffracted by a series of parallel atomic planes. The Bragg diffraction condition has much wider applications than just crystallography; for example, it is of central importance to the operation of modern semiconductor lasers.

X-ray Diffraction and Study of Crystal Structures

When an X-ray beam is incident on a single crystal, the scattered beam from a given set of planes in the crystal is at an angle 2θ that satisfies the Bragg law. In three dimensions, all directions from the crystal that are at an angle 2θ to the incident beam define a cone as shown in Figure A.3a

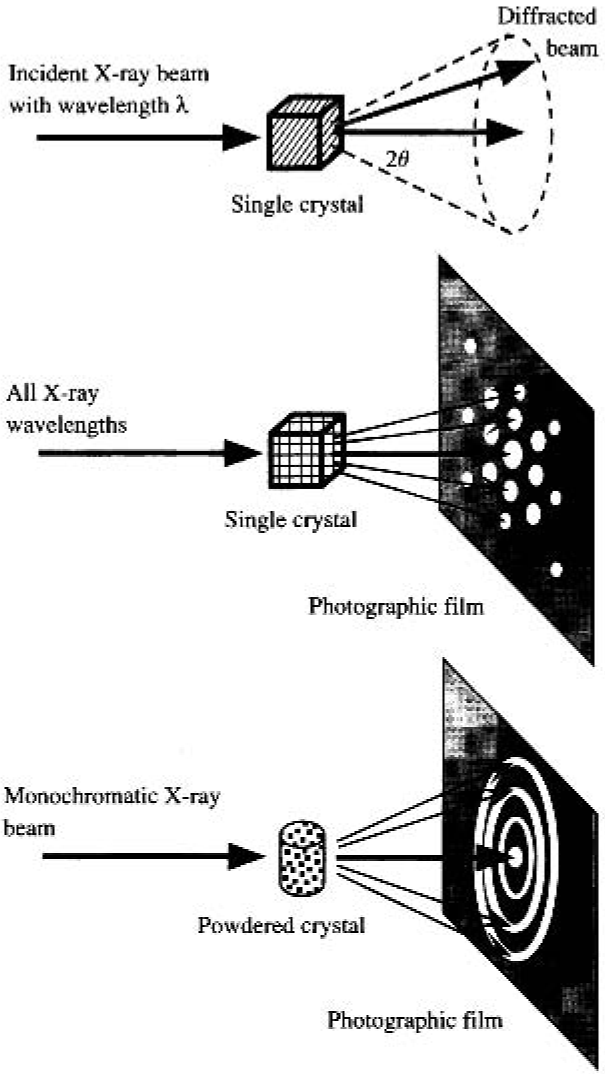

(a) All 2θ directions around the incident beam define a diffraction cone. The diffracted beam lies on the cone, but its exact direction depends on the exact orientation of the diffraction planes to the incident beam.

(b) *Laue technique.* A single crystal is irradiated with a beam of white X-rays. Diffracted X-rays give a spot diffraction pattern on a photographic plate.

(c) *Powdered crystal technique.* A sample of powdered crystal is irradiated with a monochromatic (single wavelength) X-ray beam. Diffracted X-rays give diffraction rings on a photographic plate.

Figure A.3

with its apex at the crystal. This is called a *diffraction cone.* There are many such diffraction cones, each corresponding to a different set of diffraction planes with a distinct set of Miller indices (*hkl*). Although all lines lying on a diffraction cone satisfy the Bragg condition, the exact direction of the diffracted beam depends on the exact orientation (or tilt) of the diffracting planes to the incident ray. When a monochromatic X-ray beam is incident on a single crystal, as illustrated in Figure A.3a, the diffracted beam is along one particular direction on the diffraction cone for that set of diffraction planes (*hkl*) with a particular orientation to the incident beam.

The **Laue technique** of studying crystal structures involves irradiating a single crystal with a white X-ray beam that has a wide range of wavelengths. A photographic plate is used to capture the diffraction pattern as shown in Figure A.3b. Effectively we are scanning the wavelength λ and picking up diffractions from various (hkl) planes each time the Bragg condition is satisfied. Thus, whenever λ and d for a particular set of (hkl) planes satisfy the Bragg condition, there is a diffraction. The diffraction pattern is a spot pattern where each spot is the result of diffraction from a given set of (hkl) planes oriented in a particular way to the incident beam. By using a range of wavelengths we ensure that the required wavelength is available for obtaining diffraction for a given set of planes. The relative positions of the spots are used to determine the crystal structure.

One of the simplest methods for studying crystal structures is the **powder technique** which involves irradiating a powdered crystal, or a polycrystalline sample, with a collimated X-ray beam of known wavelength (monochromatic) as shown in Figure A.3c. Powdering the crystal enables a given set of (hkl) planes to receive the X-rays at many different angles θ and at many different orientations, or tilts. Put differently, it allows the angle θ to be scanned for differently oriented crystals. Since all possible crystal orientations are present by virtue powdering, the diffracted rays form diffraction cones and the diffraction pattern developed on a photographic plate has *diffraction rings* as shown in Figure A.3c.

Each diffraction ring in the powder technique in Figure A.3c represents diffraction from a given set of (hkl) planes. Whenever the angle θ satisfies the Bragg law for a given set of atomic planes, with Miller indices (hkl) and with an interplanar separation d_{hkl}, there is a diffracted beam. An X-ray detector placed at an angle 2θ with respect to the through-beam will register a peak in the detected X-ray intensity, as shown in Figure A.4a. The instrument that allows this type of X-ray diffraction study is called a **diffractometer.** The variation of the detected intensity with the diffraction angle 2θ represents the diffraction pattern of the crystal. The particular diffraction pattern depicted in Figure A.4b is for aluminum, an FCC crystal. Different crystals exhibit different diffraction patterns.

In the case of cubic crystals, the interplanar spacing d is related to the Miller indices of a plane (hkl). The separation d_{hkl} between adjacent (hkl) planes is given by

Interplanar separation in cubic crystals

$$d_{hkl} = \frac{a}{\sqrt{h^2+k^2+l^2}} \qquad \textbf{[A.2]}$$

where a is the lattice parameter (side of the cubic unit cell). When we substitute for $d = d_{hkl}$ in the Bragg condition in Equation A.1, square both sides, and rearrange the equation, we find

Bragg condition for cubic crystals

$$(\sin\theta)^2 = \frac{n^2\lambda^2}{4a^2}(h^2+k^2+l^2) \qquad \textbf{[A.3]}$$

This is essentially **Bragg's law for cubic crystals.** The diffraction angle increases with $(h^2+k^2+l^2)$. Higher-order Miller indices, those with greater values of $(h^2+k^2+l^2)$, give rise to wider diffraction angles. For example, the diffraction angle for (111) is smaller than that for (200) because $(h^2+k^2+l^2)$ is 3 for (111) and 4 for (200). Furthermore, with λ and a values that are typically involved in X-ray diffraction, second- and higher-order diffraction peaks, $n = 2, 3, \ldots$, can be ruled out.

In the case of the simple cubic crystal all possible (hkl) planes give rise to diffraction peaks with diffraction angles satisfying the Bragg law or Equation A.3. The latter equation therefore defines a diffraction pattern for the simple cubic crystal structure because it generates all the possible values of 2θ for all the planes in the cubic crystal. In the case of FCC and BCC crystals, however, not all (hkl) planes give rise to diffraction peaks predicted by Equation A.3. Examination

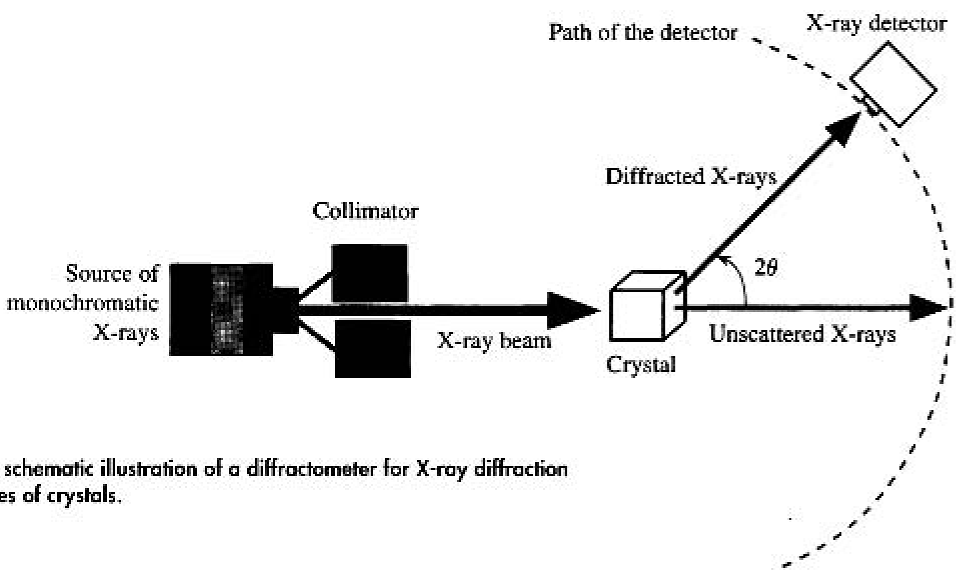

(a) A schematic illustration of a diffractometer for X-ray diffraction studies of crystals.

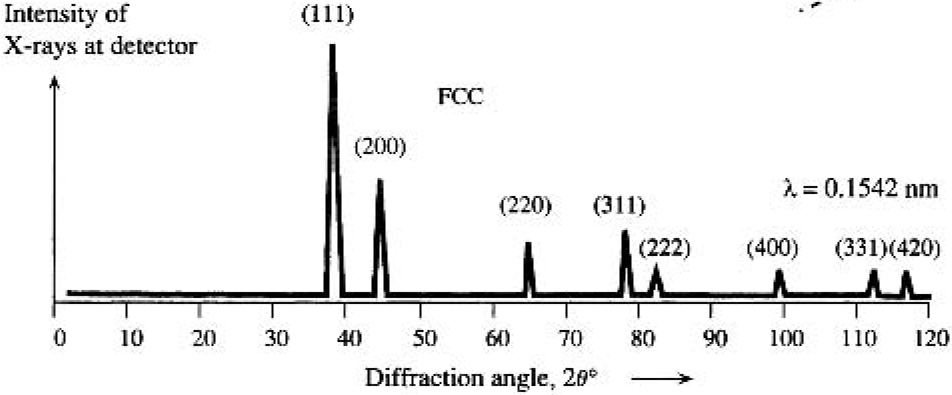

(b) A schematic diagram illustrating the intensity of X-rays as detected in (a) versus the diffraction angle, 2θ, for an FCC crystal (e.g., Al).

Figure A.4 A schematic diagram of a diffractometer and the diffraction pattern obtained from an FCC crystal.

of the diffraction pattern in Figure A.4b for an FCC crystal shows that only those planes with Miller indices that are either all odd or all even integers give rise to diffraction peaks. There are no diffractions from those planes with mixed odd and even integers.

The Bragg law for the cubic crystals in Equation A.3 is a necessary diffraction condition but not sufficient because diffraction involves the interaction of EM waves with the electrons in the crystal. To determine whether there will be a diffraction peak from a set of planes in a crystal we also have to consider the distributions of the atoms and their electrons in the crystal. In FCC and BCC structures diffractions from certain planes are missing because the atoms on these planes give rise to out-of-phase reflections.

appendix
B

Flux, Luminous Flux, and the Brightness of Radiation

Many optoelectronic light emitting devices are compared by their luminous efficiencies, which requires a knowledge of photometry. **Radiometry** is the science of radiation measurement, for example, the measurement of emitted, absorbed, reflected, transmitted radiation energy; radiation is understood to mean electromagnetic energy in the optical frequency range (ultraviolet, visible, and infrared). **Photometry,** on the other hand, is a subset of radiometry in which radiation is measured with respect to the spectral responsivity of the eye, that is, over the visible spectrum and by taking into account the spectral visual sensitivity of the eye under normal light adapted conditions, *i.e.*, *photopic* conditions.

Flux (Φ) in radiometry has three related definitions, **radiant, luminous** and **photon flux,** which correspond to the rate of flow of radiation energy, perceptible visual energy, and photons, respectively. (Notice that, in radiometry, these fluxes are not defined in terms of flow *per unit area.*) For example, **radiant flux** is the energy flow per unit time in the units of Watts. Radiometric quantities, such as *radiant flux* Φ_e, radiant energy flow per unit time, usually have a subscript e and invariably involve energy or power. Radiometric *spectral* quantities, such as *spectral radiant flux* Φ_λ, refer to the radiometric quantity per unit wavelength; *i.e.*, $\Phi_\lambda = d\Phi_e/d\lambda$ is the radiant flux per unit wavelength.

Luminous flux or **photometric flux** Φ_v, is the visual "brightness" of a source as observed by an average daylight adapted eye and is proportional to the radiant flux (radiation power emitted) of the source and the efficiency of the eye to detect the spectrum of the emitted radiation. While the eye can see a red color source, it cannot see an infrared source, and the luminous flux of the infrared source would be zero. Similarly, the eye is less efficient in the violet than in the green region, and less radiant flux is needed to have a green source at the same luminous flux as the blue source. Luminous flux Φ_v is measured in **lumens** (lm), and at a particular wavelength it is given by

$$\Phi_v = \Phi_e \times K \times \eta_{eye}$$

Luminous flux in lumens

where Φ_e is the radiant flux (in Watts), K is a conversion constant (standardized to be 633 lm/W), η_{eye} (also denoted as V) is the *luminous efficiency (luminous efficacy)* of the daylight adapted eye, which is unity at 555 nm; η_{eye} depends on the wavelength. By definition, a 1 W light source emitting at 555 nm (green, where $\eta_{eye} = 1$) emits a luminous flux of 633 lm. The same 1 W light source at 650 nm (red), where $\eta_{eye} = 0.11$, emits only 70 lm. When we buy a light bulb, we are essentially paying for lumens because it is luminous flux that the eye perceives. A typical 60 W incandescent lamp provides roughly 900 lm. Fluorescent tubes provide more luminous flux output than incandescent lamps for the same electric power input as they have more spectral emission in the visible region and make better use of the eye's spectral sensitivity. Some examples are 100 W incandescent lamps, 1300–1800 lm, depending on the filament operating temperature (hence bulb design), and 25 W compact fluorescent lamps, 1500–1750 lm.

Luminous efficacy of a light source (such as a lamp) in the lighting industry is the efficiency with which an electric light source converts the input electric power (W) into an emitted luminous flux (lm). A 100 W light bulb producing 1700 lm has an efficacy of 17 lm/W. While at present the LED efficacies are below those of fluorescent tubes, rapid advances in LED technologies are bringing the expected efficacies to around 50 lm/W or higher. LEDs as solid-state lamps have much longer lifetimes and much higher reliability, and hence are expected to be more economical than incandescent and fluorescent lamps.

From left to right: Michael Faraday, Thomas Henry Huxley, Charles Wheatstone, David Brewster and John Tyndall. Professor Tyndall has been attributed with the first demonstration (1854) of light being guided along a water jet, which is based in total internal reflection.

| SOURCE: Courtesy of AIP Emilio Segrè Visual Archives, Zeleny Collection.

appendix

C

Major Symbols and Abbreviations

A	area; cross-sectional area; amplification
a	lattice parameter; acceleration; amplitude of vibrations; half-channel thickness in a JFET (Ch. 6)
a (subscript)	acceptor, *e.g.*, N_a = acceptor concentration (m^{-3})
ac	alternating current
a_o	Bohr radius (0.0529 nm)
A_V, A_P	voltage amplification, power amplification
APF	atomic packing factor
$\mathbf{B}$, B	magnetic field vector (T), magnetic field
B	frequency bandwidth
B_c	critical magnetic field
B_m	maximum magnetic field
B_o, B_e	Richardson–Dushman constant, effective Richardson–Dushman constant
BC	base collector
BCC	body-centered cubic
BE	base emitter
BJT	bipolar junction transistor
C	capacitance; composition; the Nordheim coefficient (Ω m)
c	speed of light (3×10^8 m s^{-1}); specific heat capacity (J K^{-1} kg^{-1})
C_{dep}	depletion layer capacitance
C_m	molar heat capacity (J K^{-1} mol^{-1})
C_{diff}	diffusion (storage) capacitance of a forward-biased *pn* junction
c_s	specific heat capacity (J K^{-1} kg^{-1})
C_v	heat capacity per unit volume (J K^{-1} m^{-3})
CB	conduction band; common base
CE	common emitter
CMOS	complementary MOS
CN	coordination number
CVD	chemical vapor deposition
D	diffusion coefficient (m^2 s^{-1}); thickness; electric displacement (C m^{-2})
d	density (kg m^{-3}); distance; separation of the atomic planes in a crystal, separation of capacitor plates; piezoelectric coefficient; mean grain size (Ch. 2)

d (subscript)	donor, *e.g.*, N_d = donor concentration (m^{-3})
dc	direct current
d_{ij}	piezoelectric coefficients
E	energy; electric field (V m^{-1}) (Ch. 9)
E_a, E_d	acceptor and donor energy levels
E_c, E_v	conduction band edge, valence band edge
E_{ex}	exchange interaction energy
E_F, E_{FO}	Fermi energy, Fermi energy at 0 K
E_g	bandgap energy
E_{mag}	magnetic energy
$\mathcal{E}$	electric field (V m^{-1})
$\mathcal{E}_{\text{br}}$	dielectric strength or breakdown field (V m^{-1})
$\mathcal{E}_{\text{loc}}$	local electric field
e	electronic charge (1.602×10^{-19} C)
e (subscript)	electron, *e.g.*, μ_e = electron drift mobility; electronic
eff (subscript)	effective, *e.g.*, μ_{eff} = effective drift mobility
EHP	electron–hole pair
EM	electromagnetic
EMF (emf)	electromagnetic force (V)
F	force (N); function
f	frequency; function
$f(E)$	Fermi–Dirac function
FCC	face-centered cubic
FET	field effect transistor
G	rate of generation
G_{ph}	rate of photogeneration
G_p	parallel conductance (Ω^{-1})
$g(E)$	density of states
g	conductance; transconductance (A/V); piezoelectric voltage coefficient (Ch. 7)
g_d	incremental or dynamic conductance (A/V)
g_m	mutual transconductance (A/V)
$\mathbf{H}$, H	magnetic field intensity (strength), magnetizing field (A m^{-1})
h	Planck's constant (6.6261×10^{-34} J s)
$\hbar$	Planck's constant divided by 2π ($\hbar = 1.0546 \times 10^{-34}$ J s)
h (subscript)	hole, *e.g.*, μ_h = hole drift mobility
h_{FE}, h_{fe}	dc current gain, small-signal (ac) current gain in the common emitter configuration
HCP	hexagonal close-packed
HF	high frequency
I	electric current (A); moment of inertia (kg m^2) (Ch. 1)
$\mathcal{I}$	light intensity (W m^{-2})
I, i (subscript)	quantity related to ionic polarization
I_{br}	breakdown current
I_B, I_C, I_E	base, collector, and emitter currents in a BJT

i	instantaneous current (A); small-signal (ac) current, $i = \delta I$
i (subscript)	intrinsic, *e.g.*, n_i = intrinsic concentration
i_b, i_c, i_e	small signal base, collector, and emitter currents ($\delta I_B, \delta I_C, \delta I_E$) in a BJT
IC	integrated circuit
J	current density (A m^{-2})
$\mathbf{J}$	total angular momentum vector
	imaginary constant: $\sqrt{-1}$
J_c	critical current density (A m^{-2})
J_p	pyroelectric current density
JFET	junction FET
K	spring constant (Ch. 1); phonon wavevector (m^{-1}); bulk modulus (Pa); dielectric constant (Ch. 7)
	Boltzmann constant ($k = R/N_A = 1.3807 \times 10^{-23}$ J K^{-1}); wavenumber ($k = 2\pi/\lambda$), wavevector (m^{-1}); electromechanical coupling factor (Ch. 7)
KE	kinetic energy
$\mathbf{L}$	total orbital angular momentum
L	length; inductance
	length; mean free path; orbital angular momentum quantum number
L_{ch}	channel length in a FET
L_e, L_h	electron and hole diffusion lengths
ℓ_n, ℓ_p	lengths of the n- and p-regions outside depletion region in a pn junction
ln (x)	natural logarithm of x
LCAO	linear combination of atomic orbitals
$\mathbf{M}, M$	magnetization vector (A m^{-1}), magnetization (A m^{-1})
M	multiplication in avalanche effect
M_{at}	relative atomic mass; atomic mass; "atomic weight" (g mol^{-1})
M_r	remanent or residual magnetization (A m^{-1}); reduced mass of two bodies A and B, $M_r = M_A M_B/(M_A + M_B)$
M_{sat}	saturation magnetization (A m^{-1})
m	mass (kg)
m_e	mass of the electron in free space (9.10939×10^{-31} kg)
m_e^*	effective mass of the electron in a crystal
m_h^*	effective mass of a hole in a crystal
m_ℓ	magnetic quantum number
m_s	spin magnetic quantum number
MOS (MOST)	metal-oxide-semiconductor (transistor)
MOSFET	metal-oxide-semiconductor FET
N	number of atoms or molecules; number of atoms per unit volume (m^{-3}) (Chs. 7 and 9); number of turns on a coil (Ch. 8)
N_A	Avogadro's number (6.022×10^{23} mol^{-1})
n	electron concentration (number per unit volume); atomic concentration; principal quantum number; integer number; refractive index (Ch. 9)
n^+	heavily doped n-region
n_{at}	number of atoms per unit volume

N_c, N_v	effective density of states at the conduction and valence band edges (m^{-3})
N_d, N_d^+	donor and ionized donor concentrations (m^{-3})
n_e, n_o	refractive index for extraordinary and ordinary waves in a birefringent crystal
n_i	intrinsic concentration (m^{-3})
n_{no}, p_{po}	equilibrium majority carrier concentrations (m^{-3})
n_{po}, p_{no}	equilibrium minority carrier concentrations (m^{-3})
N_s	concentration of electron scattering centers
n_v	velocity density function; vacancy concentration (m^{-3})
P	probability; pressure (Pa); power (W) or power loss (W)
$\mathbf{p}$, p	electric dipole moment (C m)
p	hole concentration (m^{-3}); momentum (kg m s^{-1}); pyroelectric coefficient (C m^{-2} K^{-1}) (Ch. 7)
p^+	heavily doped p-region
p_{av}	average dipole moment per molecule
p_e	electron momentum (kg m s^{-1})
PE	potential energy
p_{induced}	induced dipole moment (C m)
p_o	permanent dipole moment (C m)
PET	polyester, polyethylene terephthalate
PZT	lead zirconate titanate
Q	charge (C); heat (J); quality factor
Q'	rate of heat flow (W)
q	charge (C); an integer number used in lattice vibrations (Ch. 4)
R	gas constant ($N_A k = 8.3145$ J mol^{-1} K^{-1}); resistance; radius; reflection coefficient (Ch. 3); rate of recombination (Ch. 5)
R	reflectance (Ch. 9)
$\mathcal{R}_I$, $\mathcal{R}_V$	pyroelectric current and voltage responsivities
$\mathbf{r}$	position vector
r	radial distance; radius; interatomic separation; resistance per unit length
r	reflection coefficient (Ch. 9)
R_H	Hall coefficient (m^3 C^{-1})
r_o	bond length, equilibrium separation
rms	root mean square
$\mathbf{S}$	total spin momentum, intrinsic angular momentum; Poynting vector (Ch. 9)
S	cross-sectional area of a scattering center; Seebeck coefficient, thermoelectric power (V m^{-1}); strain (Ch. 7)
S_{band}	number of states per unit volume in the band
S_j	strain along direction j
SCL	space charge layer
T	temperature in Kelvin; transmission coefficient
T	transmittance
t	time (s); thickness (m)
t	transmission coefficient
$\tan\delta$	loss tangent

T_C	Curie temperature
T_c	critical temperature (K)
T_j	mechanical stress along direction j (Pa)
TC	thermocouple
TCC	temperature coefficient of capacitance (K^{-1})
TCR	temperature coefficient of resistivity (K^{-1})
U	total internal energy
	mean speed (of electron) (m s^{-1})
V	voltage; volume; PE function of the electron, $PE(x)$
V_{br}	breakdown voltage
V_o	built-in voltage
V_P	pinch-off voltage
V_r	reverse bias voltage
v, v	velocity (m s^{-1}); instantaneous voltage (V)
$\overline{v^2}$	mean square velocity; mean square voltage
v_{dx}	drift velocity in the x direction
v_e, v_{rms}	effective velocity or rms velocity of the electron
	Fermi speed
v_g	group velocity
v_{th}	thermal velocity
VB	valence band
W	width; width of depletion layer with applied voltage; dielectric loss
W_o	width of depletion region with no applied voltage
W_n, W_p	width of depletion region on the n-side and on the p-side with no applied voltage
X	atomic fraction
Y	admittance (Ω^{-1}); Young's modulus (Pa)
Z	impedance (Ω); atomic number, number of electrons in the atom
	polarizability; temperature coefficient of resistivity (K^{-1}); absorption coefficient (m^{-1}); gain or current transfer ratio from emitter to collector of a BJT
β	current gain I_C/I_B of a BJT; Bohr magneton (9.2740×10^{-24} J T^{-1}); spring constant (Ch. 4)
β_S	Schottky coefficient
γ	emitter injection efficiency (Ch. 6); gyromagnetic ratio (Ch. 8); Grüneisen parameter (Ch. 4); loss coefficient in the Lorentz oscillator model
Γ_{ph}	flux (m^{-2} s^{-1}), photon flux (photons m^{-2} s^{-1})
	small change; skin depth (Ch. 2); loss angle (Ch. 7); domain wall thickness (Ch. 8); penetration depth (Ch. 9)
Δ	change, excess ($e.g.$, Δn = excess electron concentration)
∇^2	$\partial^2/\partial x^2 + \partial^2/\partial y^2 + \partial^2/\partial z^2$
	$\varepsilon_o\varepsilon_r$, permittivity of a medium (C V^{-1} m^{-1} or F m^{-1}); elastic strain
	permittivity of free space or absolute permittivity (8.8542×10^{-12} C V^{-1} m^{-1} or F m^{-1})

ε_r	relative permittivity or dielectric constant
η	efficiency; quantum efficiency; ideality factor
θ	angle; an angular spherical coordinate; thermal resistance; angle between a light ray and normal to a surface (Ch. 9)
κ	thermal conductivity ($\mathrm{W\ m^{-1}\ K^{-1}}$); dielectric constant
λ	wavelength (m); thermal coefficient of linear expansion ($\mathrm{K^{-1}}$); electron mean free path in the bulk crystal (Ch. 2); characteristic length (Ch. 8)
$\boldsymbol{\mu}$, μ	magnetic dipole moment ($\mathrm{A\ m^2}$) (Ch. 3)
μ	$\mu_o\mu_r$, magnetic permeability ($\mathrm{H\ m^{-1}}$); chemical potential (Ch. 5)
μ_o	absolute permeability ($4\pi \times 10^{-7}\ \mathrm{H\ m^{-1}}$)
μ_r	relative permeability
$\boldsymbol{\mu}_m$, μ_m	magnetic dipole moment ($\mathrm{A\ m^2}$) (Ch. 8)
μ_d	drift mobility ($\mathrm{m^2\ V^{-1}\ s^{-1}}$)
μ_h, μ_e	hole drift mobility, electron drift mobility ($\mathrm{m^2\ V^{-1}\ s^{-1}}$)
ν	frequency (Hz); Poisson's ratio; volume fraction (Ch. 7)
π	pi, 3.14159. . . ; piezoresistive coefficient ($\mathrm{Pa^{-1}}$)
π_L, π_T	longitudinal and transverse piezoresistive coefficients ($\mathrm{Pa^{-1}}$)
Π	Peltier coefficient (V)
ρ	resistivity (Ω m); density ($\mathrm{kg\ m^{-3}}$); charge density ($\mathrm{C\ m^{-3}}$)
ρ_E	energy density ($\mathrm{J\ m^{-3}}$)
ρ_{net}	net space charge density ($\mathrm{C\ m^{-3}}$)
ρJ^2	Joule heating per unit volume ($\mathrm{W\ m^{-3}}$)
σ	electrical conductivity ($\Omega^{-1}\ \mathrm{m^{-1}}$); surface concentration of charge ($\mathrm{C\ m^{-2}}$) (Ch. 7)
σ_P	polarization charge density ($\mathrm{C\ m^{-2}}$)
σ_o	free surface charge density ($\mathrm{C\ m^{-2}}$)
σ_S	Stefan's constant ($5.670 \times 10^{-8}\ \mathrm{W\ m^{-2}\ K^{-4}}$)
τ	time constant; mean electron scattering time; relaxation time; torque (N m)
τ_g	mean time to generate an electron–hole pair
ϕ	angle; an angular spherical coordinate
Φ	work function (J or eV), magnetic flux (Wb)
Φ_e	radiant flux (W)
Φ_m	metal work function (J or eV)
Φ_n	energy required to remove an electron from an n-type semiconductor (J or eV)
Φ_v	luminous flux (lumens)
χ	volume fraction; electron affinity; susceptibility (χ_e is electrical; χ_m is magnetic)
$\Psi\ (x, t)$	total wavefunction
$\psi(x)$	spatial dependence of the electron wavefunction under steady-state conditions
$\psi_k(x)$	Bloch wavefunction, electron wavefunction in a crystal
ψ_{hyb}	hybrid orbital
ω	angular frequency ($2\pi\nu$); oscillation frequency ($\mathrm{rad\ s^{-1}}$)
ω_I	ionic polarization resonance frequency (angular)
ω_o	resonance or natural frequency (angular) of an oscillating system.

appendix

D

Elements to Uranium

Element	Symbol	Z	Atomic Mass (g mol^{-1})	Electronic Structure	Density (g cm^{-3}) (*at 0 °C, 1 atm)	Crystal in Solid State
Hydrogen	H	1	1.008	$1s^1$	0.00009*	HCP
Helium	He	2	4.003	$1s^2$	0.00018*	FCP
Lithium	Li	3	6.941	$[He]2s^1$	0.54	BCC
Beryllium	Be	4	9.012	$[He]2s^2$	1.85	HCP
Boron	B	5	10.81	$[He]2s^2p^1$	2.5	Rhombohedral
Carbon	C	6	12.01	$[He]2s^2p^2$	2.3	Hexagonal
Nitrogen	N	7	14.007	$[He]2s^2p^3$	0.00125*	HCP
Oxygen	O	8	16.00	$[He]2s^2p^4$	0.00143*	Monoclinic
Fluorine	F	9	18.99	$[He]2s^2p^5$	0.00170*	Monoclinic
Neon	Ne	10	20.18	$[He]2s^2p^6$	0.00090*	FCC
Sodium	Na	11	22.99	$[Ne]3s^1$	0.97	BCC
Magnesium	Mg	12	24.31	$[Ne]3s^2$	1.74	HCP
Aluminum	Al	13	26.98	$[Ne]3s^2p^1$	2.70	FCC
Silicon	Si	14	28.09	$[Ne]3s^2p^2$	2.33	Diamond
Phosphorus	P	15	30.97	$[Ne]3s^2p^3$	1.82	Triclinic
Sulfur	S	16	32.06	$[Ne]3s^2p^4$	2.0	Orthorhombic
Chlorine	Cl	17	35.45	$[Ne]3s^2p^5$	0.0032*	Orthorhombic
Argon	Ar	18	39.95	$[Ne]3s^2p^6$	0.0018*	FCC
Potassium	K	19	39.09	$[Ar]4s^1$	0.86	BCC
Calcium	Ca	20	40.08	$[Ar]4s^2$	1.55	FCC
Scandium	Sc	21	44.96	$[Ar]3d^14s^2$	3.0	HCP
Titanium	Ti	22	47.87	$[Ar]3d^24s^2$	4.5	HCP
Vanadium	V	23	50.94	$[Ar]3d^34s^2$	5.8	BCC
Chromium	Cr	24	52.00	$[Ar]3d^54s^1$	7.19	BCC
Manganese	Mn	25	54.95	$[Ar]3d^54s^2$	7.43	BCC
Iron	Fe	26	55.85	$[Ar]3d^64s^2$	7.86	BCC
Cobalt	Co	27	58.93	$[Ar]3d^74s^2$	8.90	HCP
Nickel	Ni	28	58.69	$[Ar]3d^84s^2$	8.90	FCC
Copper	Cu	29	63.55	$[Ar]3d^{10}4s^1$	8.96	FCC
Zinc	Zn	30	65.39	$[Ar]3d^{10}4s^2$	7.14	HCP
Gallium	Ga	31	69.72	$[Ar]3d^{10}4s^2p^1$	5.91	Orthorhombic
Germanium	Ge	32	72.61	$[Ar]3d^{10}4s^2p^2$	5.32	Diamond

Element	**Symbol**	**Z**	**Atomic Mass ($\mathrm{g\ mol^{-1}}$)**	**Electronic Structure**	**Density ($\mathrm{g\ cm^{-3}}$) (*at 0 °C, 1 atm)**	**Crystal in Solid State**
Arsenic	As	33	74.92	[Ar]$3d^{10}4s^2p^3$	5.72	Rhombohedral
Selenium	Se	34	78.96	[Ar]$3d^{10}4s^2p^4$	4.80	Hexagonal
Bromine	Br	35	79.90	[Ar]$3d^{10}4s^2p^5$	3.12	Orthorhombic
Krypton	Kr	36	83.80	[Ar]$3d^{10}4s^2p^6$	3.74	FCC
Rubidium	Rb	37	85.47	[Kr]$5s^1$	1.53	BCC
Strontium	Sr	38	87.62	[Kr]$5s^2$	2.6	FCC
Yttrium	Y	39	88.90	[Kr]$4d^15s^2$	4.5	HCP
Zirconium	Zr	40	91.22	[Kr]$4d^25s^2$	6.50	HCP
Niobium	Nb	41	92.91	[Kr]$4d^45s^1$	8.55	BCC
Molybdenum	Mo	42	95.94	[Kr]$4d^55s^1$	10.2	BCC
Technetium	Tc	43	(97.91)	[Kr]$4d^55s^2$	11.5	HCP
Ruthenium	Ru	44	101.07	[Kr]$4d^75s^1$	12.2	HCP
Rhodium	Rh	45	102.91	[Kr]$4d^85s^1$	12.4	FCC
Palladium	Pd	46	106.42	[Kr]$4d^{10}$	12.0	FCC
Silver	Ag	47	107.87	[Kr]$4d^{10}5s^1$	10.5	FCC
Cadmium	Cd	48	112.41	[Kr]$4d^{10}5s^2$	8.65	HCP
Indium	In	49	114.82	[Kr]$4d^{10}5s^2p^1$	7.31	FCT
Tin	Sn	50	118.71	[Kr]$4d^{10}5s^2p^2$	7.30	BCT
Antimony	Sb	51	121.75	[Kr]$4d^{10}5s^2p^3$	6.68	Rhombohedral
Tellurium	Te	52	127.60	[Kr]$4d^{10}5s^2p^4$	6.24	Hexagonal
Iodine	I	53	126.91	[Kr]$4d^{10}5s^2p^5$	4.92	Orthorhombic
Xenon	Xe	54	131.29	[Kr]$4d^{10}5s^2p^6$	0.0059*	FCC
Cesium	Cs	55	132.90	[Xe]$6s^1$	1.87	BCC
Barium	Ba	56	137.33	[Xe]$6s^2$	3.62	BCC
Lanthanum	La	57	138.91	[Xe]$5d^16s^2$	6.15	HCP
Cerium	Ce	58	140.12	[Xe]$4f^15d^16s^2$	6.77	FCC
Praseodymium	Pr	59	140.91	[Xe]$4f^36s^2$	6.77	HCP
Neodymium	Nd	60	144.24	[Xe]$4f^46s^2$	7.00	HCP
Promethium	Pm	61	(145)	[Xe]$4f^56s^2$	7.26	Hexagonal
Samarium	Sm	62	150.4	[Xe]$4f^66s^2$	7.5	Rhombohedral
Europium	Eu	63	151.97	[Xe]$4f^76s^2$	5.24	BCC
Gadolinium	Gd	64	157.25	[Xe]$4f^75d^16s^2$	7.90	HCP
Terbium	Tb	65	158.92	[Xe]$4f^96s^2$	8.22	HCP
Dysprosium	Dy	66	162.50	[Xe]$4f^{10}6s^2$	8.55	HCP
Holmium	Ho	67	164.93	[Xe]$4f^{11}6s^2$	8.80	HCP
Erbium	Er	68	167.26	[Xe]$4f^{12}6s^2$	9.06	HCP
Thulium	Tm	69	168.93	[Xe]$4f^{13}6s^2$	9.32	HCP
Ytterbium	Yb	70	173.04	[Xe]$4f^{14}6s^2$	6.90	FCC
Lutetium	Lu	71	174.97	[Xe]$4f^{14}5d^16s^2$	9.84	HCP
Hafnium	Hf	72	178.49	[Xe]$4f^{14}5d^26s^2$	13.3	HCP
Tantalum	Ta	73	180.95	[Xe]$4f^{14}5d^36s^2$	16.4	BCC
Tungsten	W	74	183.84	[Xe]$4f^{14}5d^46s^2$	19.3	BCC
Rhenium	Re	75	186.21	[Xe]$4f^{14}5d^56s^2$	21.0	HCP

Element	Symbol	Z	Atomic mass (g mol^{-1})	Electronic Structure	Density (g cm^{-3}) (*at 0 °C, 1 atm)	Crystal in Solid State
Osmium	Os	76	190.2	$[Xe]4f^{14}5d^{6}6s^{2}$	22.6	HCP
Iridium	Ir	77	192.22	$[Xe]4f^{14}5d^{7}6s^{2}$	22.5	FCC
Platinum	Pt	78	195.08	$[Xe]4f^{14}5d^{9}6s^{1}$	21.4	FCC
Gold	Au	79	196.97	$[Xe]4f^{14}5d^{10}6s^{1}$	19.3	FCC
Mercury	Hg	80	200.59	$[Xe]4f^{14}5d^{10}6s^{2}$	13.55	Rhombohedral
Thallium	Tl	81	204.38	$[Xe]4f^{14}5d^{10}6s^{2}p^{1}$	11.8	HCP
Lead	Pb	82	207.2	$[Xe]4f^{14}5d^{10}6s^{2}p^{2}$	11.34	FCC
Bismuth	Bi	83	208.98	$[Xe]4f^{14}5d^{10}6s^{2}p^{3}$	9.8	Rhombohedral
Polonium	Po	84	(209)	$[Xe]4f^{14}5d^{10}6s^{2}p^{4}$	9.2	SC
Astatine	At	85	(210)	$[Xe]4f^{14}5d^{10}6s^{2}p^{5}$	—	—
Radon	Rn	86	(222)	$[Xe]4f^{14}5d^{10}6s^{2}p^{6}$	0.0099*	Rhombohedral
Francium	Fr	87	(223)	$[Rn]7s^{1}$	—	—
Radium	Ra	88	226.02	$[Rn]7s^{2}$	5	BCC
Actinium	Ac	89	227.02	$[Rn]6d^{1}7s^{2}$	10.0	FCC
Thorium	Th	90	232.04	$[Rn]6d^{2}7s^{2}$	11.7	FCC
Protactinium	Pa	91	(231.03)	$[Rn]5f^{2}6d^{1}7s^{2}$	15.4	BCT
Uranium	U	92	(238.05)	$[Rn]5f^{3}6d^{1}7s^{2}$	19.07	Orthorhombic

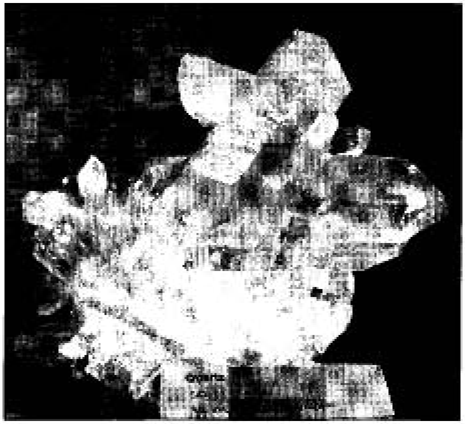

"I don't really start until I get my proofs back from the printers. Then I can begin serious writing."

John Maynard Keynes (1883–1946)

appendix

E

Constants and Useful Information

Physical Constants

Atomic mass unit	amu	1.66054×10^{-27} kg
Avogadro's number	N_A	6.02214×10^{23} mol^{-1}
Bohr magneton	β	9.2740×10^{-24} J T^{-1}
Boltzmann constant	k	1.3807×10^{-23} J K^{-1} $= 8.6174 \times 10^{-5}$ eV K^{-1}
Electron mass in free space	m_e	9.10939×10^{-31} kg
Electron charge	e	1.60218×10^{-19} C
Gas constant	R	8.3145 J K^{-1} mol^{-1} or m^3 Pa K^{-1} mol^{-1}
Gravitational constant	G	6.6742×10^{-11} N m^2 kg^{-2}
Permeability of vacuum or absolute permeability	μ_o	$4\pi \times 10^{-7}$ H m^{-1} (or Wb A^{-1} m^{-1})
Permittivity of vacuum or absolute permittivity	ε_o	8.8542×10^{-12} F m^{-1}
Planck's constant	h	6.626×10^{-34} J s $= 4.136 \times 10^{-15}$ eV s
Planck's constant$/2\pi$	$\hbar$	1.055×10^{-34} J s $= 6.582 \times 10^{-16}$ eV s
Proton rest mass	m_p	1.67262×10^{-27} kg
Rydberg constant	R_∞	1.0974×10^{7} m^{-1}
Speed of light	c	2.9979×10^{8} m s^{-1}
Stefan's constant	σ_s	5.6704×10^{-8} W m^{-2} K^{-4}

Useful Information

Acceleration due to gravity at 45° latitude	g	9.81 m s^{-2}
kT at $T = 293$ K (20 °C)	kT	0.02525 eV
kT at $T = 300$ K (27 °C)	kT	0.02585 eV
Bohr radius	a_o	0.0529 nm
1 angstrom	Å	10^{-10} m
1 micron	μm	10^{-6} m

1 eV $= 1.6022 \times 10^{-19}$ J

1 kJ mol^{-1} $= 0.010364$ eV atom^{-1}

1 atmosphere (pressure)
$= 1.013 \times 10^{5}$ Pa

LED Colors

The table gives the wavelength ranges and colors as usually specified for LEDs.

Color	Blue	Emerald green	Green	Yellow	Amber	Orange	Red orange	Red	Deep red	Infrared
λ (nm)	$\lambda < 500$	530–564	565–579	580–587	588–594	595–606	607–615	616–632	633–700	$\lambda > 700$

Visible Spectrum

The table gives the typical wavelength ranges and color perception by an average person.

Color	Violet	Blue	Green	Yellow	Orange	Red
λ (nm)	390–455	455–492	492–577	577–597	597–622	622–780

Complex Numbers

$j = (-1)^{1/2} \qquad j^2 = -1$

$\exp(j\theta) = \cos\theta + j\sin\theta$

$Z = a + jb = re^{j\theta} \qquad r = (a^2 + b^2)^{1/2} \qquad \tan\theta = \frac{b}{a}$

$Z^* = a - jb = re^{-j\theta} \qquad \mathrm{Re}(Z) = a \qquad \mathrm{Im}(Z) = b$

$\text{Magnitude}^2 = |Z|^2 = ZZ^* = a^2 + b^2 \qquad \text{Argument} = \theta = \arctan\left(\frac{b}{a}\right)$

$\cos\theta = \frac{1}{2}(e^{j\theta} + e^{-j\theta}) \qquad \sin\theta = \frac{1}{2j}(e^{j\theta} - e^{-j\theta})$

Expansions

$$e^x = 1 + x + \frac{1}{2!}x^2 + \frac{1}{3!}x^3 + \cdots$$

$$(1+x)^n = 1 + nx + \frac{n(n-1)}{2!}x^2 + \frac{n(n-1)(n-2)}{3!}x^3 + \cdots$$

Small x: $(1+x)^n \approx 1 + nx \qquad \sin x \approx x \qquad \tan x \approx x \qquad \cos x \approx 1$

Small Δx in $x = x_o + \Delta x$: $f(x) \approx f(x_o) + \Delta x\left(\frac{df}{dx}\right)_{x_o}$